UFSM

CIÊNCIA e NATURA

ISSN 2179-460X
OPEN ACCESS

Ci. e Nat., Santa Maria, v. 46, e85441, 2024 • https://doi.org/10.5902/2179460X85441
Submitted: 17/10/2023 • Approved: 27/09/2024 • Published: 06/12/2024

Geo-Sciences

How has deforestation affected and might affect the climate in the Amazon basin during the rainy season?

Como o desflorestamento tem afetado e poderá afetar o clima da bacia Amazônica durante a estação chuvosa?

Karoline Suelly de Souza Mendes[I], Adriane Lima Brito[I], Adriana Lira Lima[I], José Augusto Paixão Veiga[I]

[I] Universidade do Estado do Amazonas, Manaus, AM, Brazil

ABSTRACT

Changes in land use and land cover in the Amazon rainforest, whether due to natural or anthropogenic causes, are occurring at increasingly rapid rates, with potential implications for regional climate. Therefore, studies aiming to understand the effects of deforestation on the Amazon basin are becoming highly necessary. The main objective of this study was to understand, through regional numerical modeling, how deforestation has been affecting and may affect in the future the spatial pattern of precipitation and temperature in the Amazon basin during the rainy season. To achieve this, data from numerical experiments with different spatial scales of deforestation in the Amazon were used. These data were generated by the regional ETA model forced by the HadGEM2-ES model for a 30-year period. The analyses were performed in the form of climate anomalies. For the current climate, the results indicate that a scenario of partial deforestation would lead to significant increases in temperature and a slight local increase in precipitation in the Arc of Deforestation region. On the other hand, a scenario in which the entire Amazon Forest is removed showed more prominent increases in temperature and reductions in precipitation throughout the Amazon basin.

Keywords: Deforestation; Regional modeling climate; Climate changes

RESUMO

Mudanças no uso e na cobertura do solo da floresta Amazônica, seja por causas naturais ou antropogênicas, estão ocorrendo a taxas cada vez mais crescentes, podendo afetar o clima regional. Assim sendo, estudos que visam compreender os efeitos do desflorestamento sobre a bacia Amazônica tornam-se cada vez mais necessários. O presente estudo teve como objetivo principal entender, por meio de modelagem numérica regional, como o desflorestamento tem afetado e poderá afetar futuramente o padrão espacial da precipitação e da temperatura na bacia Amazônica durante o período chuvoso.

Para tanto, foram utilizados dados de experimentos numéricos com distintas escalas espaciais de desflorestamento na Amazônia. Estes dados foram gerados a partir do modelo regional ETA forçado a partir do modelo HadGEM2-ES para um período de 30 anos. As análises foram realizadas em forma de anomalias climáticas. Para o clima atual, os resultados indicam que um cenário de desflorestamento parcial ocasionaria mudanças intensas do aumento da temperatura e um pequeno aumento local da precipitação na região do Arco de Desflorestamento. Por outro lado, um cenário no qual foi removida toda a floresta Amazônica mostrou mudanças mais intensas do aumento da temperatura e da redução da precipitação sobre toda a área da bacia Amazônica.

Palavras-chave: Desflorestamento; Modelagem regional do clima; Mudanças do clima

1 INTRODUCTION

The Amazon region comprises a set of ecosystems with rich biodiversity and intense convective activity, with an average precipitation of around 2,300 mm.year-1 (Marengo, 2006). Located in the tropics, the Amazon rainforest is considered the largest continuous expanse of tropical rainforest ecosystem on the planet (Durieux et al., 2003). The region plays an important role in the exchange of heat, moisture, and momentum at the surface-atmosphere interface, which is crucial for maintaining the dynamic and thermodynamic balance between climate and vegetation (Nobre et al., 1991). Furthermore, the Amazon forest acts as a global climate regulator by balancing water, energy, and biogeochemical processes (Alves et al., 2017).

Despite its intense hydrological cycle, the region is vulnerable to variability and changes in the components of the climate system, whether due to natural causes or human activity (Correia et al., 2008; Marengo & Espinoza, 2016). Any changes in land cover or vegetation can alter the fluxes of heat, moisture, and momentum that affect the pattern of atmospheric circulation (Shukla et al., 1990), the hydrological cycle (Alves et al., 2017), energy and carbon balances (de Brito Gomes et al., 2020), and the average temperature of the Amazon basin (Nobre et al., 2007).

The conversion of forest cover to pasture and agricultural crops is occurring at alarming rates, with particular emphasis on the expansion of degraded pasture for livestock and soybean production (Rocha et al., 2014). According to estimates from the

Satellite Monitoring of Deforestation in Legal Amazon Project – PRODES (INPE, 2022), the intensity of clear-cut deforestation has significantly increased since 2015. The PRODES data also revealed that the accelerated rate of deforestation in the Amazon reached approximately 11,568 km² in 2021, representing a reduction of 11.27% compared to the deforestation rate corresponding to 2020, which was approximately 13,038 km². In light of these findings, conducting research aimed at understanding the effects of deforestation on regional climate is becoming increasingly necessary.

Numerical modeling studies on the climate of the Amazon basin reveal that changes in forest surface impact the regional climate by directly altering the average regional values of temperature and precipitation (Costa & Pires, 2010; Artaxo et al., 2014). Several studies (Lean & Warrilow, 1989; Shukla et al., 1990; Dickinson & Kennedy, 1992; Nobre et al., 1991; Lean & Rowntree, 1997; Costa & Foley, 2000; Sampaio et al., 2007; Eiras-Barca et al., 2020; Sampaio et al., 2020) have used global numerical models to assess the effects of deforestation on the climate of the Amazon basin. In general, the results have shown similar effects for scenarios where the Amazon forest is replaced by degraded pasture, such as increased surface temperature, decreased evapotranspiration, and reduced precipitation.

Other studies have also observed similar effects on the climate of the Amazon basin using regional numerical models (Correia et al., 2008; Lejeune et al., 2015; Silva et al., 2016; Llopart et al., 2018). Eltahir and Bras (1994) found that small-scale deforestation (~250 km) reduced surface net radiation, evaporation, and precipitation, resulting in increased surface temperature. The results from Gandu et al. (2004) demonstrated that partial deforestation impacts on the climate of the eastern portion of the Amazon basin led to negative latent heat anomalies and positive sensible heat anomalies during the dry season. Consequently, the authors observed reductions in moisture convergence and precipitation, as well as an increase in surface temperature for the same season.

Thus, numerical modeling studies aiming to assess the impacts of deforestation on the climate of the Amazon basin have enabled the quantification of imbalances, magnitudes, and damages that deforestation can cause to Amazonian ecosystems, primary sectors of agriculture, the economy, and vulnerable communities in the region (Doughty et al., 2015). They also help establish concrete measures to reduce the more severe consequences associated with ongoing deforestation in the coming decades. Therefore, the present study aims to understand, through numerical modeling, how deforestation has affected and may further affect the spatial pattern of precipitation and temperature over the Amazon basin, specifically during the rainy season.

2 METHODS

2.1 Description of the Study Area

The study area corresponds to the region of the Amazon River basin, which has a drainage area of approximately 6.1 million km² (figure 1) and an average annual precipitation of 2,300 mm (Salati et al., 1979; Marengo, 2006). The precipitation regime in the region is strongly influenced by meteorological systems of different spatial and temporal scales, such as the Intertropical Convergence Zone, South Atlantic Convergence Zone, Bolivian High, lines of instability, convective clusters, among others (de Oliveira & Fitzjarrald 1994; Mota & Souza, 1996; Reboita et al., 2010). The rainy season spans from December to May, while the dry season corresponds to the period from June to November (Ananias et al., 2010). The climate classification is of the humid tropical type, and the average annual temperatures range from 24 °C to 26 °C (Limberger & Silva, 2016).

Figure 1 – Map of the Amazon basin boundary

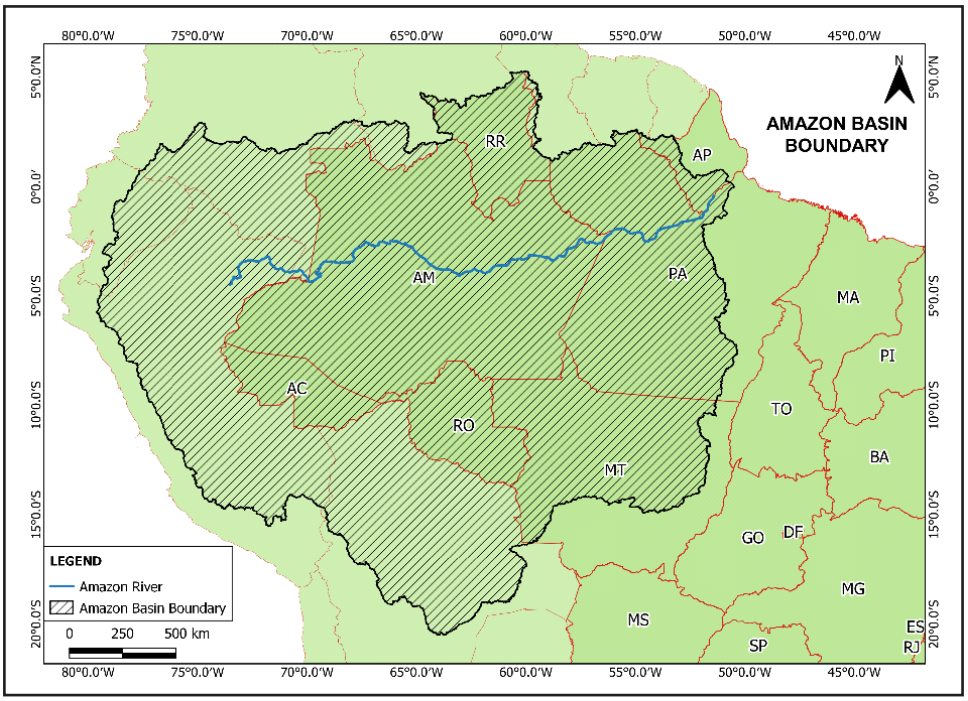

Source: Authors' private collection (May 2022)

2.2 Numerical models used

In the present study, data from numerical experiments using the mesoscale ETA model forced by initial and boundary conditions from the global HadGEM2-ES model were utilized through the technique of dynamic downscaling. To understand how the spatial scale of deforestation affects and may alter the future spatial pattern of precipitation and temperature during the rainy season in the Amazon basin, three numerical simulations were conducted with the ETA model: one controlled experiment and two sensitivity experiments.

2.1.1 Global model HadGEM2-ES

The Hadley Centre Global Environmental Model Version 2 (HadGEM2-ES) is a coupled atmosphere-ocean numerical model of the Earth system. This model was developed by the UK Met Office to understand and simulate climate aspects in conjunction with biological factors, in order to obtain better simulations of various

processes within the climate system (Collins et al., 2011). The Earth System components of this model ("ES") incorporate atmospheric chemistry and the terrestrial and oceanic carbon cycles (Bellouin et al., 2011).

The atmospheric component of the model has a spatial resolution of approximately 1.875° (longitude) by 1.25° (latitude), with 38 vertical levels extending over a height of more than 39 km. The oceanic component uses a horizontal grid of 0.33°×0.33°, with a spacing of 1° and 30° between the poles. The grid is gradually refined to 1/3° and 1×1° at latitudes above 30° and has 40 vertical levels (Collins et al., 2011). The land carbon cycle is modeled using the TRIFFID (Top-down Representation of Interactive Foliage Including Dynamics) vegetation dynamics, as described by Cox (2001). Over the ocean, the Diat-HadOCC ocean biology model (Palmer & Totterdell, 2001) represents the carbon cycle. The atmospheric chemistry is based on the UKCA (UK Chemistry and Aerosols) tropospheric chemistry scheme (O'Connor et al., 2014). The model incorporates atmospheric chemical processes such as organic carbon from fossil fuel, ammonia nitrate, dust, and biogenic organic aerosols (Bellouin et al., 2011). HadGEM2-ES distinguishes five types of plants, including trees with broad and thin leaves, C3 and C4 type grasses, and shrubs. The model uses a 30-minute time step for the atmospheric and surface components, and a 1-hour time step for the oceanic component. Detailed descriptions of the second version of the HadGEM2-ES model can be found in Bellouin et al. (2011).

This model has been applied in studies assessing the impacts of climate change in the Amazon (Rocha, 2016; Rocha et al., 2019) by using emission scenarios and land use changes regionalized for South America through the use of the ETA regional climate model.

2.1.2 Regional climate model ETA/CPTEC

The ETA model is a regional atmospheric model developed by the National Center for Environmental Prediction (NCEP) and the University of Belgrade, and has

been improved since 1996 by researchers at the Center for Weather Forecasting and Climate Studies of the National Institute for Space Research (CPTEC/INPE) (Mesinger et al., 2012). The model is used to simulate the evolution of the atmospheric field at various spatial and temporal scales for weather forecasting and climate studies. ETA is a grid-point model based on the ETA vertical coordinate (η), which is sensitive in mountainous areas, making it suitable for studies in regions with steep topography such as the Andes mountain range in South America (Mesinger, 1984). Currently, it is one of the models used to quantify the impacts of deforestation and greenhouse gas emissions on the climate of the Amazon and South America (Rodriguez et al., 2014; Fonseca et al., 2017; Brito et al., 2019; de Brito Gomes et al., 2020).

The physical parameterizations used in the model were as follows: the turbulent diffusion scheme in the Planetary Boundary Layer, described by Mellor and Yamada (1974); shortwave and longwave radiation schemes according to Fels and Schwarzkopf (1975) and Lacis and Hansen (1974), respectively. Precipitation in the model was parameterized by the cumulus schemes proposed by Betts-Miller (Betts & Miller, 1986), and cloud microphysics followed the scheme proposed by Zhao et al. (1997). Surface processes were parameterized using the NOAH scheme (Ek et al., 2003), which includes 4 soil layers (surface to the deepest layer: 10, 30, 60, and 100 cm) for temperature and humidity, and distinguishes 12 vegetation types and 7 soil types.

In this study, simulations with the ETA model were conducted for a continuous 30-year period (00 UTC on January 1, 1974, to 18 UTC on December 31, 2004). Due to the model's spin-up effect, the first year of the simulations was discarded, resulting in an evaluation period of 29 years. The model was configured with a resolution of 40 km, 38 vertical levels, and a top level at 50 hPa. The integration domain covered South America and parts of Central America (50°S-27.8°N; 100°W-29°W), but only the area

of interest for this study was analyzed. The model was also adapted to assimilate sea surface temperature (SST) data derived from monthly averages of the HadGEM2-ES model.

2.3 Description of the numerical experiments

For the control experiment, a vegetation map without deforested areas (FLOR) was considered, representing an intact forest area of the entire Amazon biome (Sestini et al., 2002). The first sensitivity experiment, referred to as DF15, was characterized by the current deforestation condition in the Amazon according to the deforestation scenario relative to the year 2015 (Sestini et al., 2002). The second sensitivity experiment, named DFTOT, was based on a total deforestation condition estimated for the year 2100 (Sestini et al., 2002). As analyzed in other studies (Eltahir and Brás, 1994; Gandu et al., 2004; Correia et al., 2008; Silva et al., 2016; de Brito Gomes et al., 2020), deforestation in this study was established by replacing forested areas in the Amazon basin with degraded pasture areas (grasses) in the numerical integrations with the ETA model.

The vegetation maps for the FLOR, DF15, and DFTOT experiments were generated using the DINAMICA model (1×1 km resolution) from the ProVeg Project (Sestini et al., 2002) with data from the Project for the Estimation of Gross Deforestation in the Amazon - PRODES-DIGITAL (Sestini et al., 2002; INPE, 2017; de Brito Gomes et al., 2020). The DINAMICA landscape model is a simulation model that captures the dynamics of land use and land cover changes in the Amazon basin (Soares-Filho et al., 2004). The three vegetation maps are presented in figure 2. The scenario for the year 2015 (figure 2b) indicates a region in the eastern portion of the Amazon where deforestation expansion is more significant for degraded pastureland (black square; latitudes: 1°S to 9°S, longitudes: 42°W to 53°W).

The results were evaluated in terms of climatic anomalies by determining the difference between the sensitivity and control experiments (DF15-FLOR and DFTOT-

FLOR). In the analysis, the rainy season corresponds to the months of December to May (DJFMAM). The spatial fields of net radiation and energy fluxes anomalies (sensible and latent heat) at the surface were assessed to understand temperature-related changes. On the other hand, water budget components (evapotranspiration and moisture convergence flux) were analyzed to understand changes in the precipitation field. The spatial anomaly fields presented in the results section, corresponding to the difference between the DF15-FLOR experiments, also highlight the domain indicated by a square in the eastern portion of the Amazon (indicated by a red square).

Figure 2 – Maps of vegetation cover used in the simulations with the ETA model. (a) Vegetation cover map for the FLOR control experiment, (b) Current vegetation map for the 2015 deforestation scenario in the DF15 sensitivity experiment, and (c) Deforestation map for the year 2100 used in the DFTOT sensitivity experiment

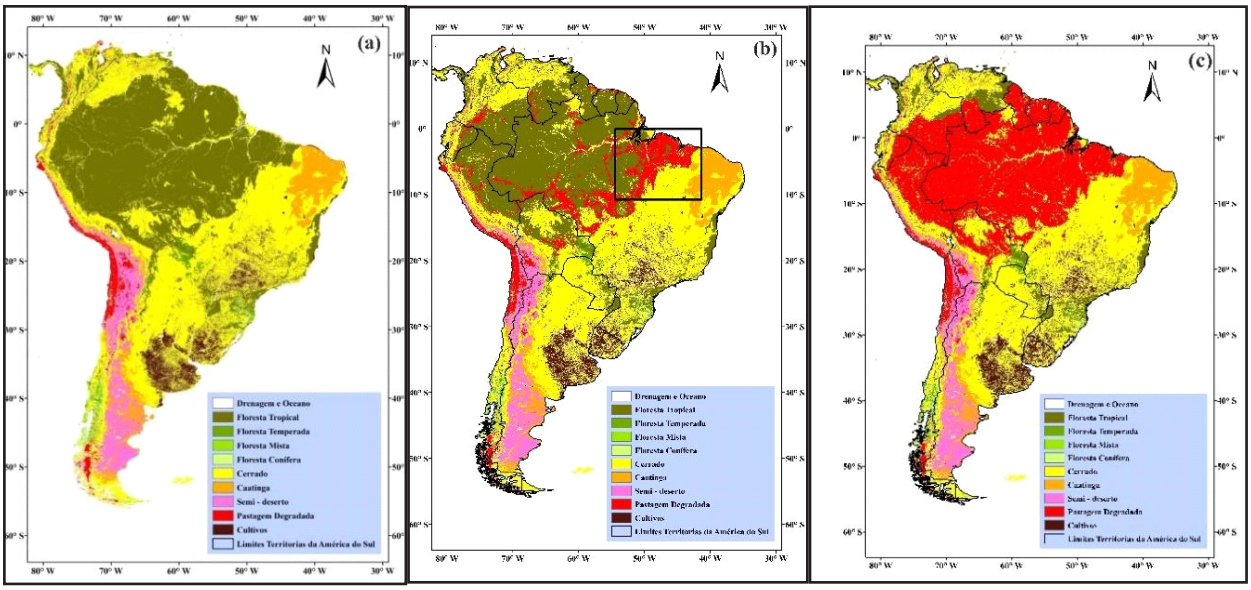

Source: Sestini et al., (2002); INPE (2017), de Brito Gomes et al., (2020)

Legend: Colors green (forest), yellow (savanna), blue (water), and red (degraded pasture). The black square represents the delimited area where the expansion of deforestation in the vegetation cover map for the 2015 scenario is greater for degraded pasture cover

3 RESULTS

3.1 Climate anomalies for a partial deforestation scenario on the Amazon basin climate

3.1.1 Surface net radiation and surface energy fluxes

The spatial fields of net radiation anomalies and sensible and latent heat fluxes at the surface for the rainy season are presented in figure 3. Negative anomalies (ranging from -1 to -10 W.m-^{2}) for the net radiation are observed in the southern, southeastern, and eastern sectors of the Amazon basin, with some areas of positive anomalies distributed in the western sector of the region (figure 3a). Positive anomalies in the sensible heat flux are also observed at certain points distributed among the southern, southeastern, and eastern sectors of the Amazon basin (figure 4b). Areas in the eastern portion of the Amazon and between the states of Rondônia and Mato Grosso show regions of negative anomalies in the latent heat flux (figure 3c).

According to these results, the replacement of forest by degraded pasture areas in the extent of the Arc of Deforestation reduced the net radiation during the rainy season in this region. One explanation for this is that the decrease in surface roughness length and the increase in surface albedo associated with the forest-to-pasture conversion are factors that can reduce the net radiation, as observed by Correia et al. (2008) and Eiras-Barca (2020). However, other factors such as greater loss of longwave radiation at the surface and reduced cloudiness (not shown) can also contribute to the reduction in surface net radiation. Additionally, the reduction in surface roughness length and the drier surface condition result in a decrease in average latent heat flux and an increase in average sensible heat flux in degraded pasture areas (Gandu et al., 2004).

Figure 3 – Anomalies between the DF15-FLOR experiments for the rainy season (DJFMAM): (a) surface net radiation (W.m-²), (b) surface sensible heat flux (W.m-²), and (c) surface latent heat flux (W.m-²)

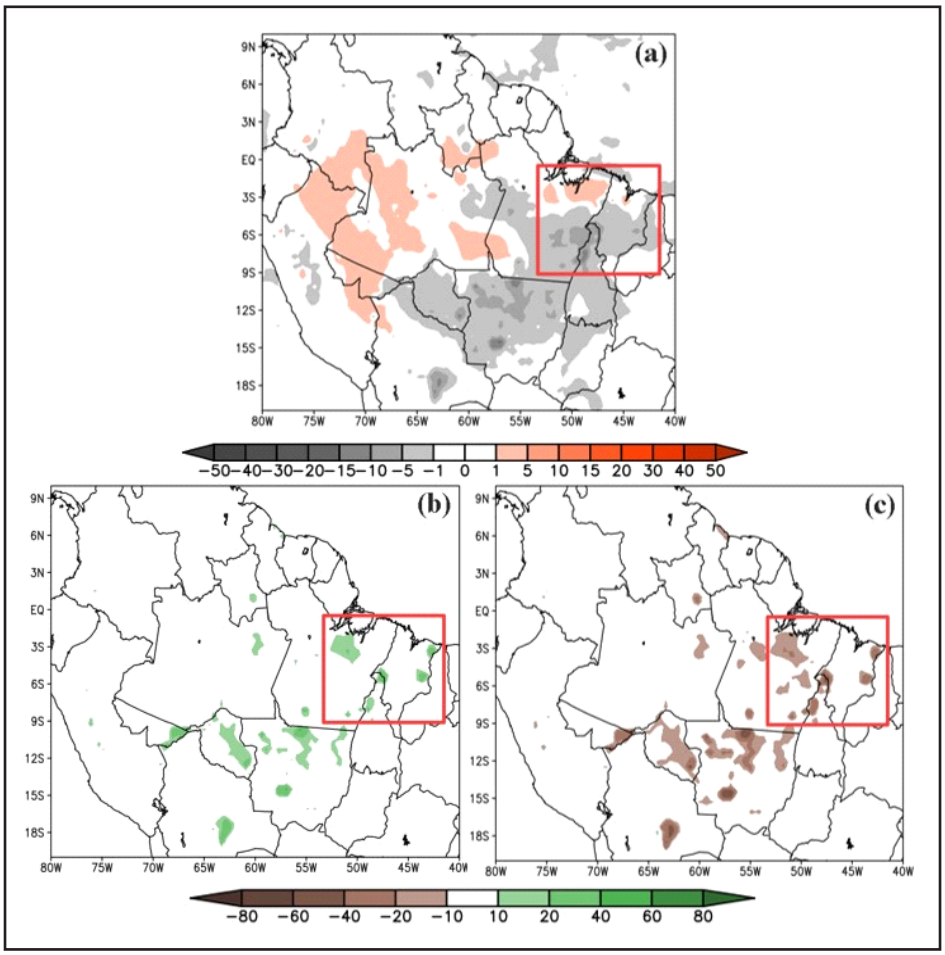

Source: Authors' private collection (May 2022).
Legend: The red square represents the delimited area where the expansion of deforestation in the vegetation cover map for the 2015 scenario is greater for degraded pasture soil

3.1.2 Temperature

The temperature anomaly fields (figure 4) for the rainy season in the Amazon basin are presented in this section. More intense positive temperature anomalies at the surface occur in the eastern sectors of the Amazon (red square) and between the states of Rondônia and Mato Grosso, with an average increase of 1° C to 4° C in the eastern, southern, and southeastern sectors of the Amazon (figure 4a). Positive

anomalies in 2-meter temperature are observed over the Amazon basin area (figure 4b), with fluctuations around 1° C to 2° C in the eastern portion of the Amazon (red square). Positive anomalies in maximum and minimum temperatures are also observed with broader coverage and intensity in the Arc of Deforestation region (figures 4c and 4d). The average temperature increases in the field are associated with changes in the availability of soil energy and are directly influenced by surface physical processes. The reduction in surface roughness length for the current scenario of Amazon deforestation dominates the observed changes in surface net radiation and energy fluxes, resulting in average positive temperature anomalies (at 2 meters) of up to 4° C (3° C). The reduction in surface net radiation and soil moisture deficit (not shown) in degraded pasture causes a portion of the available surface energy to be used for heating the boundary layer over the Arc of Deforestation region. As a result, the increase in terrestrial radiation emission (not shown) contributes to the increase in sensible heat flux and consequently the average temperature in the Arc of Deforestation region. The reduction in latent heat flux leads to a warmer and drier atmosphere (Eiras-Barca et al., 2020).

On the other hand, the increase in sensible heat flux also contributes to the average temperature increase, further accentuated by the energy exchange between the land surface and the atmosphere. Therefore, the warming effect observed in the Arc of Deforestation region is consistent with the reduction in surface roughness length in the region, as surface roughness plays a fundamental role in determining energy fluxes and exchanges of heat and moisture between the surface and the atmosphere. Similar impacts on temperature in the southern, southeastern, and eastern sectors of the Amazon basin have also been observed in climate numerical modeling studies (Sampaio et al., 2007; Gandu et al., 2004; Correia et al., Silva et al., 2016).

Figure 4 – Anomalies between the DF15-FLOR experiments for the rainy season (DJFMAM): (a) surface temperature (°C), (b) temperature at 2 meters (°C), (c) maximum temperature (°C), and (d) minimum temperature (°C)

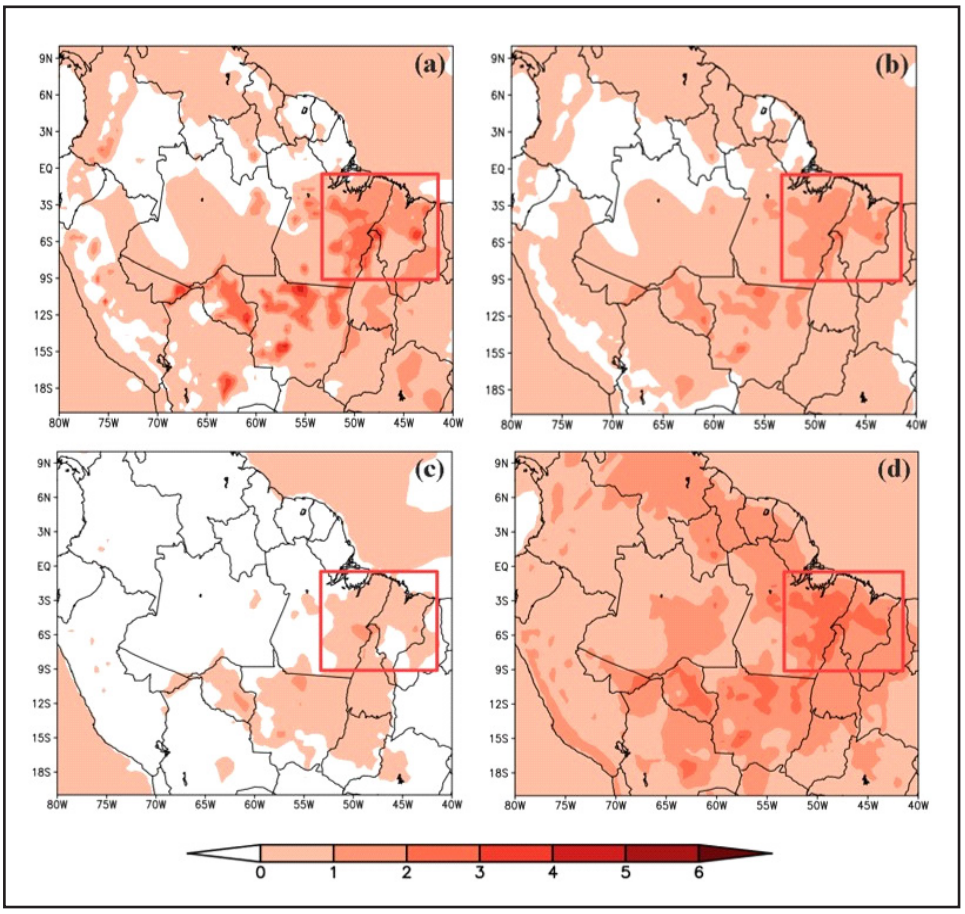

Source: Authors' private collection (May 2022)

Legend: The red square represents the delimited area where the expansion of deforestation in the vegetation cover map for the 2015 scenario is greater for degraded pasture soil

Moreover, studies such as da Silva et al. (2023) have also demonstrated an increase in surface temperature intensity and maximum temperature in the southern and eastern sectors of the Amazon, based on satellite data, as effects of the expansion of deforestation observed in recent years in areas typically allocated for agricultural production. Other studies (Chaddad et al., 2022; Butt et al., 2023) have also verified through remote sensing that continuous forest loss over the past two decades in the Amazon biome has led to an increase in surface temperature in the southern and eastern portions of the Amazon (Arc of Deforestation) and in some areas with the

presence of intact forest in the region. Similar effects of regional warming were observed in the study by Gash and Nobre (1997) through observed data from climatological measurements of experimental sites located in the Brazilian Amazon. In this study, the authors observed changes in the surface radiation and energy balance in degraded pasture areas, resulting in high surface temperatures.

3.1.3 Water budget components

Figure 5 presents the average fields of evapotranspiration (ET) and moisture convergence (estimated as the difference between precipitation and evapotranspiration, P-ET) anomalies during the rainy season. Small areas of negative ET anomalies are observed over Bolivia and between the states of Rondônia and Mato Grosso, with spatially distributed patterns (figure 5a). However, prominent negative ET anomalies are not observed in the eastern sector of the Amazon region (red square). Regarding the spatial distribution of moisture convergence anomalies, small areas of positive anomalies are observed in the Arc of Deforestation region, with limited distribution in the eastern sector of the Amazon (figure 5b).

The negative ET anomalies are a result of reduced surface roughness length and shallower root depth in degraded pasture soils with moisture deficits (de Brito Gomes et al., 2020). However, the average reduction in ET observed in figure 5a is compensated by the average increase in moisture convergence in the Arc of Deforestation region (figure 5b). Similar effects were observed by Correia et al., 2008, who found that the atmosphere acted to mitigate the effects of reduced ET through increased moisture convergence in a scenario of partial deforestation in the Amazon basin.

Figure 5 – Anomalies between the DF15-FLOR experiments for the rainy season (DJFMAM): (a) evapotranspiration (mm.day-¹) and (b) moisture convergence flux (mm.day-¹)

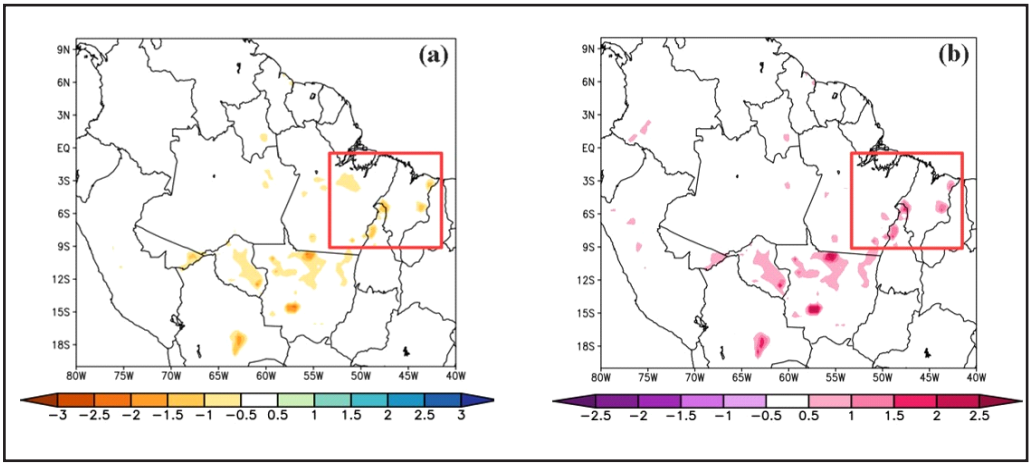

Source: Authors' private collection (May 2022)

Legend: The red square represents the delimited area where the expansion of deforestation in the vegetation cover map for the 2015 scenario is greater for degraded pasture soil

3.1.4 Precipitation

In terms of local effects, small areas of positive and negative precipitation anomalies are observed over the Amazon basin (figure 6). A slight increase in precipitation is noticeable in localized areas where deforestation rates are higher, such as in the Arc of Deforestation region. The reduction in evapotranspiration balanced by the increase in moisture convergence, discussed in the previous section, resulted in a small increase in precipitation (~0.5 mm.day-¹) in distributed areas within the Arc of Deforestation region. However, da Silva et al. (2019) demonstrated a reduction in precipitation in deforested regions over the past two decades in their analysis of spatial variability of precipitation in the Brazilian Amazon using satellite data. Remote sensing studies (Aragão et al., 2008; Leite-Filho et al., 2019; Mu et al., 2022) have also shown the impacts of deforestation on the climate of the Brazilian Amazon, with the intensifying of droughts and delays in the onset of the rainy season in regions with increasing rates of clear-cutting intensity (Arc of Deforestation). Leite-Filho et al. (2020) also showed, based on observed data from rain gauge stations, that the effects of land use changes

and Amazon forest cover on precipitation seasonality can lead to intense alterations in the amount of energy available for convection and, consequently, a reduction in precipitation during the rainy season in the southern and southeastern portions of the Amazon. Other studies using rain gauge data have also shown similar impacts of continuous deforestation in the Amazon biome on precipitation (S. Debortoli et al., 2015; Debortoli et al., 2016; O'Connor et al., 2021; Moreira et al., 2024).

Figure 6 – Precipitation anomaly (mm.day-¹) (DF15-FLOR) for the rainy season (DJFMAM)

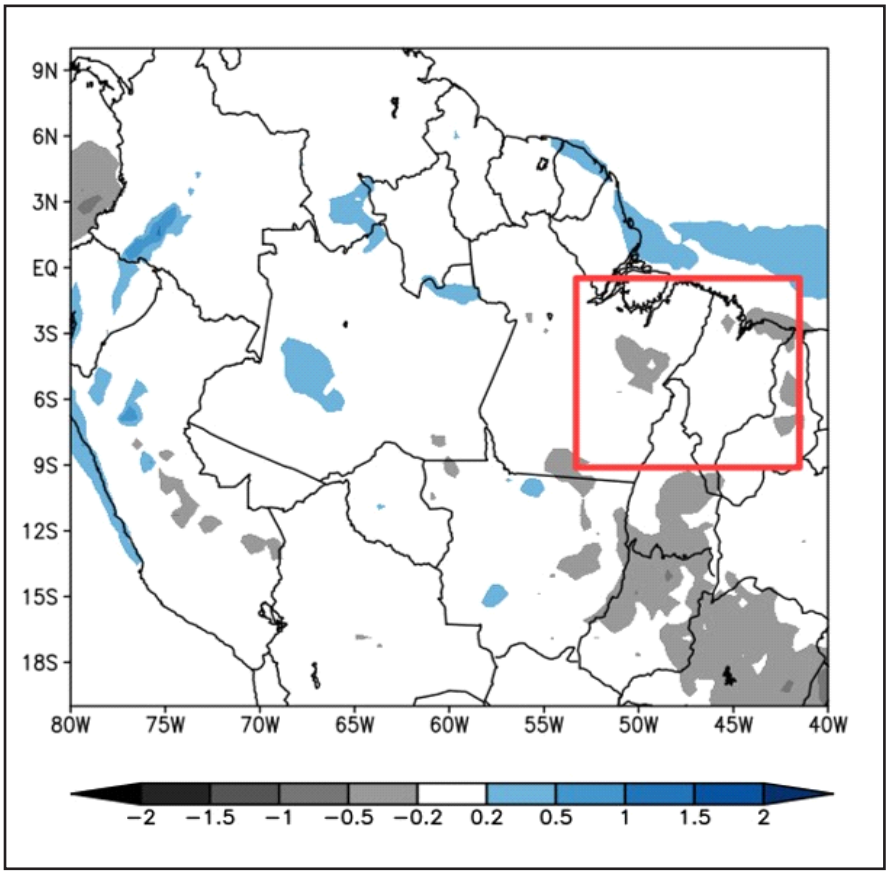

Source: Authors' private collection (May 2022)
Legend: The red square represents the delimited area where the expansion of deforestation in the vegetation cover map for the 2015 scenario is greater for degraded pasture soil

On the other hand, de Oliveira et al. (2018) observed an increase in precipitation in small areas of deforested sectors of the Amazon biome and intense reductions in larger deforested areas based on a combination of remote sensing data and meteorological stations. Correia et al. (2008) also observed localized precipitation increases in the study for a scenario of partial deforestation in the southern, southeastern, and eastern

portions of the Amazon. Therefore, the atmosphere acted to mitigate the effects of partial deforestation in specific areas of degraded pasture by increasing moisture transport, compensating for the reduced local contribution of evapotranspiration to precipitation in deforested areas.

3.1.5 Means of climate anomalies for a partial deforestation scenario

The absolute means of surface net radiation anomalies, surface energy fluxes, temperatures, water budget components, and precipitation are shown in table 1. Average values are presented for the entire Amazon basin area and for the region of interest defined by the red square in the spatial anomaly fields between the DF15 and FLOR experiments. Therefore, it is possible to understand how partial deforestation in the region spatially affects the current climate of the Amazon basin and the current climate of a smaller area in the eastern portion of the Amazon with degraded pasture cover during the rainy season.

Table 1 – Absolute means of anomalies between the DF15-FLOR experiments for surface variables of the partial deforestation scenario. Values in parentheses correspond to the mean for the area delimited by the red square in the spatial fields of climate anomalies

SURFACE VARIABLES	RAINY SEASON
Surface net radiation (W.m-²)	-0.44 (-1.74)
Sensible heat flux (W.m-²)	0.67 (2.03)
Latent heat flux (W.m-²)	-1.62 (-4.55)
Surface temperature (°C)	0.24 (0.80)
Temperature at 2 meters (°C)	0.21 (0.65)
Maximum temperature (°C)	0.23 (0.51)
Minimum temperature (°C)	0.20 (0.71)
Evapotransporation (ET) (mm.dia-¹)	-0.06 (-0.16)
Moisture convergence (P-ET) (mm.dia-¹)	0.02 (0.16)
Precipitation (mm.dia-¹)	-0.01 (0.03)

Source: Authors' private collection (May 2022)

In general, average changes in surface net radiation are larger for a deforested region (table 1). It is noted that the surface net radiation underwent a smaller reduction when considering the entire spatial scale of the Amazon basin (-0.44 W.m-²) compared to the region where all vegetation was replaced by degraded pasture (-1.74 W.m-²). Due to the reduction in surface net radiation, the average changes in sensible and latent heat fluxes were also more prominent for the region with degraded pasture cover in the eastern Amazon (2.04 W.m-² and -4.55 W.m-², respectively). The average surface temperature (at 2 meters) during the rainy season was +0.80 ° C (+0.65 ° C) in the delimited area in the eastern portion of the Amazon in terms of anomaly. Over the Amazon basin area, the expansion of deforestation for the year 2015 resulted in absolute average anomalies of surface and 2-meter temperatures of +0.24 ° C and +0.21 ° C, respectively.

Table 1 also shows that the average reduction in ET was compensated by the average increase in moisture convergence (P-ET), mainly in the delimited region for analysis in the eastern portion of the Amazon. Thus, the distinct thermal conditions in the eastern sector of the Amazon between the forest and degraded pasture induced a mesoscale circulation that transported moisture to the deforested region. As a result, the average increase in precipitation was 0.03 mm.day-¹ for the same region in terms of anomaly. However, the results presented in this section of absolute anomaly averages for the Amazon basin area (forest and degraded pasture areas) are relatively small, as the roughness length is reduced only for degraded pasture areas.

3.2 Climate anomalies for a complete deforestation scenario on the Amazon basin climate

3.2.1 Surface net radiation and surface energy fluxes

The spatial fields of net radiation anomalies and sensible and latent heat fluxes at the surface for the rainy season are presented in figure 7. Prominent regions of negative surface net radiation anomalies are observed in the state of Amazonas (ranging

from -10 to -30 W.m-²) and in the southern and southeastern sectors of the Amazon basin (figure 7a). Some areas of positive surface net radiation anomalies are observed in the extreme northeast of the state of Amazonas and in the eastern portion of the Amazon basin. An average increase in sensible heat flux occurs between the western and eastern sectors of the Amazon basin, with areas of maximum positive anomaly between the states of Amazonas, Roraima, and Pará (with variations between 40 and 80 W.m-²) (figure 7b). Average reductions in latent heat flux (negative anomalies) are observed in the Amazon basin area (figure 7c), except for specific areas in the western portion that do not exhibit anomalous variations.

Figure 7 – Anomalies between the DF15-FLOR experiments for the rainy season (DJFMAM): (a) surface net radiation (W.m-²), (b) surface sensible heat flux (W.m-²), and (c) surface latent heat flux (W.m-²)

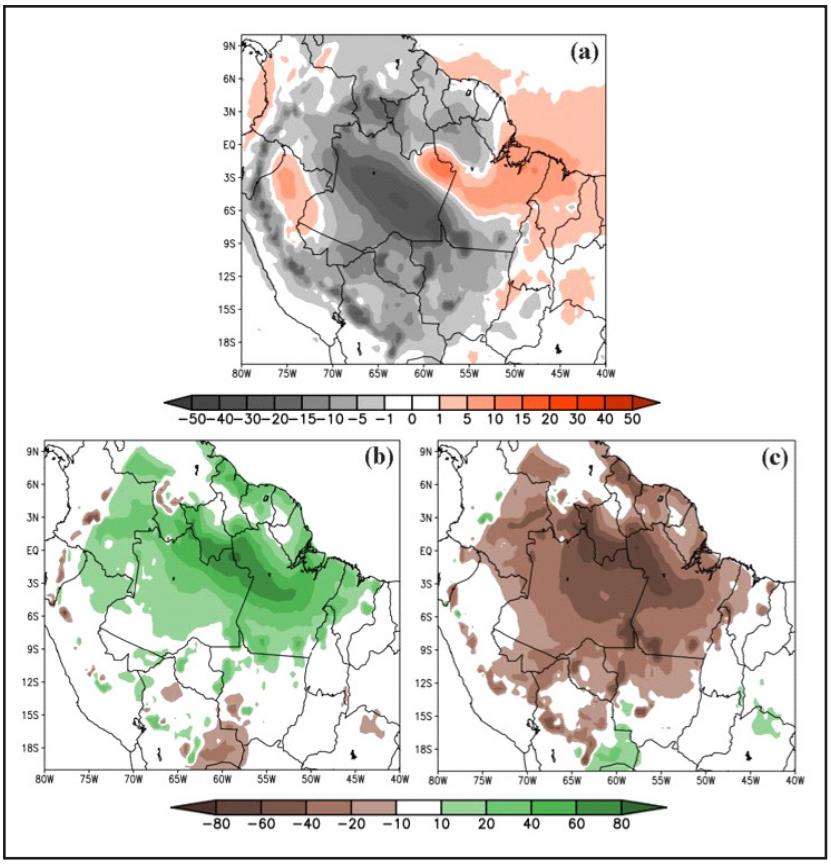

Source: Authors' private collection (May 2022)

The decrease in surface roughness length and the increase in albedo for degraded pasture soil reduces the surface net radiation during the rainy season in the Amazon basin. Similar effects of reduced surface net radiation have been observed in climate numerical modeling studies of the Amazon (Shukla et al., 1990; Nobre et al., 1991). However, factors associated with increased solar radiation incidence at the surface due to reduced cloudiness (not shown) and increased longwave radiation emitted by the surface (not shown) may outweigh the albedo increase in reducing the surface net radiation (Dickinson & Kennedy, 1992). Greater losses of longwave radiation emitted by the surface may accentuate positive anomalies in sensible heat flux in the case of complete deforestation of the Amazon basin. The lower leaf area index (not shown) and soil moisture deficit can lead to a decrease in latent heat flux (negative anomalies).

3.2.2 Temperature

Spatial fields of temperature anomalies for the rainy season in the Amazon basin are presented in this section. Positive anomalies of surface temperature, temperature at 2 meters, maximum and minimum temperatures are observed across the spatial scale of the Amazon basin with average variations ranging from 1° C to 6° C (figure 8). More prominent changes in surface temperature occur between the states of Amazonas, Roraima, and Pará, with variations between 4° C and 6° C (figure 8a). Positive anomalies of temperature at 2 meters also range from 4° C to 6° C in the northeastern portion of the Amazon basin (figure 8b). Positive trends in maximum and minimum temperature anomalies are also observed for the scenario of complete deforestation of the Amazon basin during the rainy season (figure 8c and 8d).

The average temperature increases presented in this section (positive anomalies) indicate that changes in surface energy fluxes can lead to temperature increases of up to 6° C across the entire Amazon basin during the rainy season. Despite the reduction in surface net radiation, part of the available surface energy is used to increase the sensible

heat flux and, consequently, the projected temperature increase for the condition of complete deforestation of the Amazon basin. The reduction in latent heat flux and evaporative cooling contribute to the enhanced warming in the region. Similar effects on temperature in the Amazon basin have been observed in climate modeling studies with complete replacement of forest by degraded pasture soil in numerical experiments (Lean & Warrilow, 1989; Shukla et al., 1990; Nobre et al., 1991; Lean & Rowntree, 1993; Sampaio et al., 2007; Correia et al., 2008; da Silva et al., 2008; Llopart et al., 2018).

Figure 8 – Anomalies between the DF15-FLOR experiments for the rainy season (DJFMAM): (a) surface temperature (°C), (b) temperature at 2 meters (°C), (c) maximum temperature (°C), and (d) minimum temperature (°C)

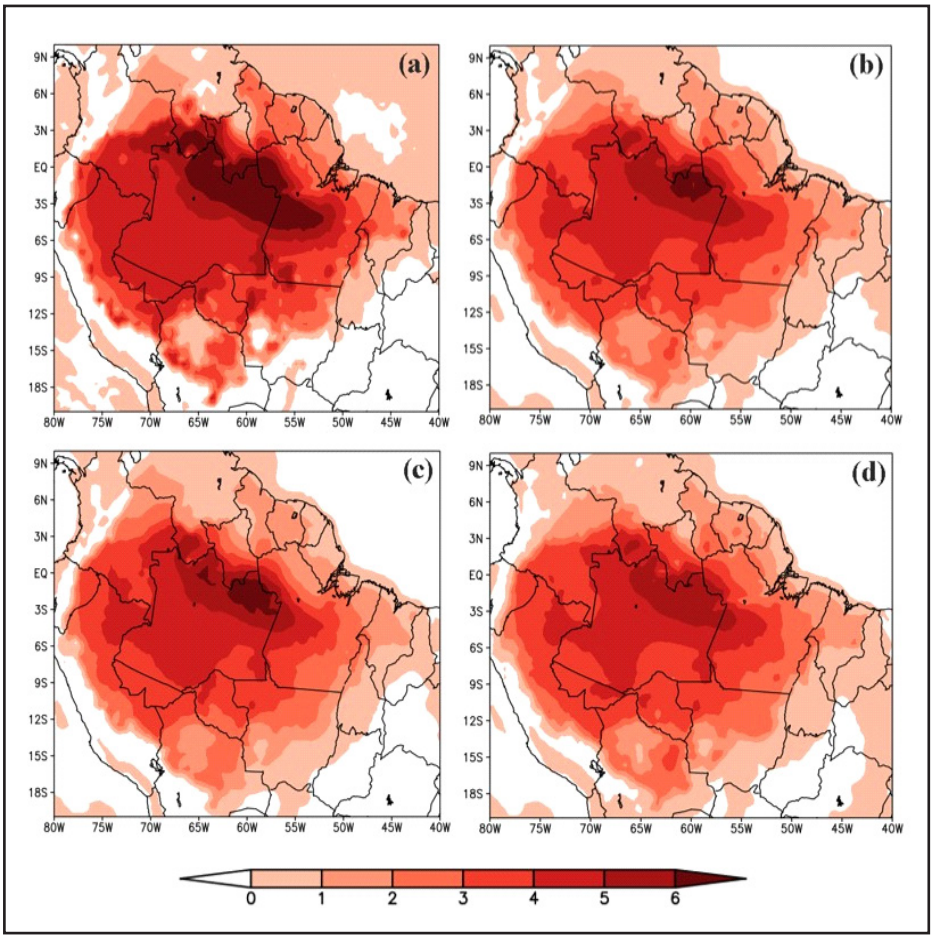

Source: Authors' private collection (May 2022)

3.2.3 Water budget components

Figure 9 presents the average spatial fields of ET and P-ET (moisture convergence) anomalies for the rainy season. Negative trends of ET anomalies are spatially distributed over the eastern portion of the Amazon (figure 9a), with maximum negative anomalies primarily located in the southern region of the Amazon basin. Intense positive anomalies of moisture convergence are observed in areas of the southern sector of the Amazon basin, ranging from 1.5 mm.day-¹ to 2 mm.day-¹ (figure 9b).

The observed changes in the spatial fields of ET and P-ET anomalies for the rainy season indicate that, in a scenario of complete deforestation of the Amazon basin, the atmosphere can act to mitigate the effects of reduced evapotranspiration by increasing the moisture convergence. Thus, the regions with maximum negative ET anomalies correspond to the areas of projected average increase in P-ET for the condition of complete deforestation of the Amazon basin (figure 9).

Figure 9 – Anomalies between the DF15-FLOR experiments for the rainy season (DJFMAM): (a) evapotranspiration (mm.day-¹) and (b) moisture convergence flux (mm. day-¹)

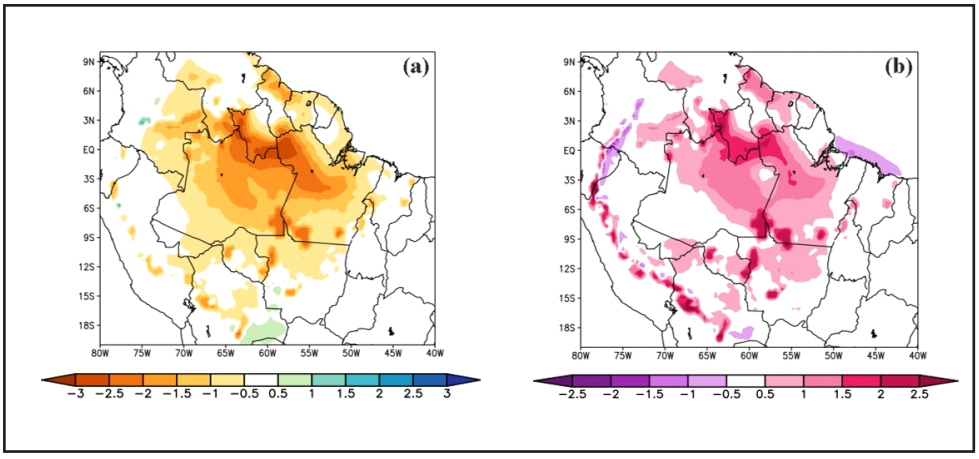

Source: Authors' private collection (May 2022)

3.2.4 Precipitation

The spatial field of precipitation anomaly for the rainy season is presented in figure 10. Over the Amazon basin, areas with west to east negative precipitation anomalies are observed, ranging from -0.2 mm.day-¹ to -1 mm.day-¹. It is noteworthy that despite the increase in P-ET in figure 9, said increase is not significant enough to balance the reduction in ET, resulting in decreased precipitation over the region. The increase in moisture convergence was only sufficient to cause a small increase in precipitation (0.5 mm.day-¹) in localized areas of the Amazon basin. Although precipitation is reduced in the scenario of complete deforestation of the region, its decrease is much smaller than the reduction in ET during the rainy season. Therefore, the significant reduction in ET may lead to a decrease in precipitation over the Amazon basin. Systematic errors of positive anomalies over the Andes are also observed in figure 10, indicating that the ETA model has limitations in simulating precipitation in steep regions.

Figure 10 – Precipitation anomaly (mm.day-¹) (DF15-FLOR) for the rainy season (DJFMAM)

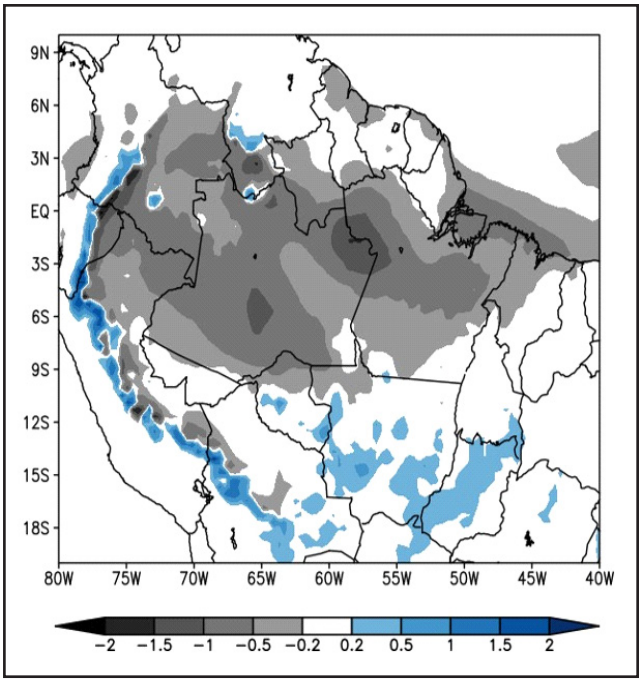

Source: Authors' private collection (May 2022)

3.2.5 Means of climate anomalies for a complete deforestation scenario

The absolute means of surface net radiation anomalies, surface energy fluxes, temperatures, water budget components, and precipitation are presented in table 2. The average values are shown for the complete deforestation spatial scale of the Amazon basin during the rainy season.

Table 2 – Absolute means of anomalies between the DFTOT-FLOR experiments for surface variables of the complete deforestation scenario

SURFACE VARIABLES	RAINY SEASON
Surface net radiation (W.m-²)	-7.57
Sensible heat flux (W.m-²)	18.82
Latent heat flux (W.m-²)	-27.09
Surface temperature (°C)	4.09
Temperature at 2 meters (°C)	3.35
Maximum temperature (°C)	3.29
Minimum temperature(°C)	3.27
Evapotranspiratiion (ET) (mm.dia-¹)	-0.96
Moisture convergence (P-ET) (mm.dia-¹)	0.60
Precipitation (mm.dia-¹)	-0.35

Source: Authors' private collection (May 2022)

The surface net radiation experienced an average reduction in negative anomaly of approximately -7.57 W.m-². As discussed earlier, factors such as reduced roughness length, increased albedo, decreased cloudiness, and greater losses of longwave radiation balance (not shown) are potential causes for the average reduction in surface net radiation (negative anomalies). This reduction led to an average increase in sensible heat flux (18.82 W.m-²) and an average decrease in latent heat flux at the surface (-27.09 W.m-²). These changes in soil energy availability resulted in an average temperature increase across the entire Amazon basin. The surface temperature

(2 meters) experienced an increase of approximately 4.09 ° C (3.35 ° C) in terms of absolute anomaly means.

Table 2 also indicates that the average increase in P-ET, approximately 0.60 mm.day-¹, was not sufficient to compensate for the reduction in ET (-0.96 mm.day-¹) in the Amazon basin area. Thus, the increased moisture transport to the region did not lead to an increase in precipitation during the rainy season. The absolute mean anomaly of precipitation for the considered season was -0.35 mm.day-¹. Although the absolute mean reduction in precipitation is small over the complete deforestation area of the Amazon basin, at local scales, the reduction in precipitation ranged from -0.2 mm.day-¹ to -1.5 mm.day-¹ (figure 10). Therefore, the complete replacement of the Amazon forest with degraded pastureland may result in a drier atmosphere with reduced rainfall volume for the climate, under complete deforestation conditions during the rainy season in the region.

4 CONCLUSIONS

The impacts of deforestation on the climate of the Amazon basin, considering two distinct deforestation scenarios, were evaluated using numerical simulations with the regional ETA model forced with initial, and boundary conditions from the global HadGEM2-ES model. Numerical integrations were performed for each scenario over a continuous 30-year period. The simulations were presented as climatological anomalies between the sensitivity experiments DF15 and DFTOT and the control (FLOR) for the rainy season.

It was observed that the replacement of forest with degraded pasture in the Arc of Deforestation area reduced the surface net radiation in the region. The sensible heat flux increased in some areas, while latent heat flux decreased due to the reduction in roughness length for the same region. Furthermore, changes in the net radiation and energy fluxes at the surface led to an average temperature increase in

the region where deforestation expansion in 2015 was most intense compared to the entire Amazon basin area (including forest and degraded pasture). Regarding changes in precipitation for the partial deforestation condition of the Amazon basin (DF15), small local increases in precipitation were observed in some sectors of the Arc of Deforestation. The increase in P-ET balanced the reduction in ET in local areas within the same region, but it was not sufficient to result in significant precipitation increases.

For the complete deforestation scenario of the Amazon basin (DFTOT), the results showed a reduction in surface net radiation and latent heat flux. With the complete removal of the Amazon forest in the numerical integrations for the climate under this scenario, an increase in the surface sensible heat flux was also observed. These changes led to an average temperature increase across the entire Amazon basin during the rainy season.

The observed increase in moisture flux transport over the entire deforested Amazon basin was not sufficient to compensate for the intense reduction in evapotranspiration and resulted in an increased precipitation during the rainy season. However, a small increase in precipitation was observed in local areas of the northwest and south sectors of the basin with positive anomalies.

Therefore, overall, it was found that a partial deforestation scenario cannot cause significant changes in the current climate of the rainy season across the entire Amazon basin. The partial deforestation scenario indicated intense changes in temperature increase and a small local precipitation increase only in the deforested region - the Arc of Deforestation. On the other hand, the complete deforestation scenario showed changes that are more prominent in temperature increase and precipitation reduction over the Amazon basin area for the rainy season. Thus, the results of this study indicate that a large-scale deforestation scenario for the Amazon basin can establish drier conditions with less precipitation during the rainy season in the region if deforestation rates continue to increase continuously.

ACKNOWLEDGEMENTS

To the Graduate Program in Climate and Environment (CLIAMB) at the Amazonas State University (UEA) / National Institute for Amazonian Research (INPA). To the Laboratory of Earth System Modeling (LABCLIM) at UEA for providing the computational infrastructure - Cluster Aruana, and to Tupã from CPTEC/INPE for performing the numerical simulations. The first author would like to thank the Coordination at the Improvement of Higher Education Personnel (CAPES) for the scholarship granted.

REFERENCES

Aragão, L. E. O., Malhi, Y., Barbier, N., Lima, A., Shimabukuro, Y., Anderson, L., & Saatchi, S. (2008). Interactions between rainfall, deforestation and fires during recent years in the Brazilian Amazonia. *Philosophical Transactions of the Royal Society B: Biological Sciences*, *363*(1498), 1779-1785. https://doi.org/10.1098/rstb.2007.0026

Alves, L. M., Marengo, J. A., Fu, R., & Bombardi, R. J. (2017). Sensitivity of Amazon regional climate to deforestation. *American Journal of Climate Change*, *6*(1), 75-98. https://doi.org/10.4236/ajcc.2017.61005

Ananias, D. D. S., Souza, E. B. D., Souza, P. F. S., Souza, A. M. L. D., Vitorino, M. I., Teixeira, G. M., & Ferreira, D. B. D. S. (2010). Climatologia da estrutura vertical da atmosfera em novembro para Belém-PA. *Revista Brasileira de Meteorologia*, *25*, 218-226. https://doi.org/10.1590/S0102-77862010000200006

Artaxo, P., Dias, M. A. F. D. S., Nagy, L., Luizão, F. J., Cunha, H. B. D., Quesada, C. A., ... & Krusche, A. (2014). Perspectivas de pesquisas na relação entre clima e o funcionamento da floresta Amazônica. *Ciência e Cultura*, *66*(3), 41-46. http://dx.doi.org/10.21800/S0009-67252014000300014

Bellouin, N., Collins, W. J., Culverwell, I. D., Halloran, P. R., Hardiman, S. C., Hinton, T. J., ... & Wiltshire, A. (2011). The HadGEM2 family of met office unified model climate configurations. *Geoscientific Model Development*, *4*(3), 723-757. https://doi.org/10.5194/gmd-4-723-2011

Betts, A. K., & Miller, M. J. (1986). A new convective adjustment scheme. Part II: Single column tests using GATE wave, BOMEX, ATEX and arctic air-mass data sets. *Quarterly Journal of the Royal Meteorological Society*, *112*(473), 693-709. https://doi.org/10.1002/qj.49711247308

Brito, A. L., Veiga, J. A. P., Correia, F. W., & Capistrano, V. B. (2019). Avaliação do desempenho dos modelos HadGEM2-ES e Eta a partir de indicadores de extremos climáticos de precipitação para a Bacia Amazônica. *Revista Brasileira de Meteorologia*, *34*, 165-177. https://doi.org/10.1590/0102-77863340003

Butt, E. W., Baker, J. C., Bezerra, F. G. S., von Randow, C., Aguiar, A. P., & Spracklen, D. V. (2023). Amazon deforestation causes strong regional warming. *Proceedings of the National Academy of Sciences*, *120*(45), e2309123120. https://doi.org/10.1073/pnas.2309123120

Chaddad, F., Mello, F. A., Tayebi, M., Safanelli, J. L., Campos, L. R., Amorim, M. T. A., ... & Demattê, J. A. (2022). Impact of mining-induced deforestation on soil surface temperature and carbon stocks: A case study using remote sensing in the Amazon rainforest. *Journal of South American Earth Sciences*, *119*, 103983. https://doi.org/10.1016/j.jsames.2022.103983

Collins, W. J., Bellouin, N., Doutriaux-Boucher, M., Gedney, N., Halloran, P., Hinton, T., ... & Woodward, S. (2011). Development and evaluation of an Earth-System model–HadGEM2. *Geoscientific Model Development*, *4*(4), 1051-1075. https://doi.org/10.5194/gmd-4-1051-2011

Correia, F. W. S., Alvalá, R. C. D. S., & Manzi, A. O. (2008). Modeling the impacts of land cover change in Amazonia: a regional climate model (RCM) simulation study. *Theoretical and Applied Climatology*, *93*, 225-244. https://doi.org/10.1007/s00704-007-0335-z

Costa, M. H., & Foley, J. A. (2000). Combined effects of deforestation and doubled atmospheric CO 2 concentrations on the climate of Amazonia. Journal of Climate, 13(1), 18-34. https://doi.org/10.1175/1520-0442(2000)013

Costa, M. H., & Pires, G. F. (2010). Effects of Amazon and Central Brazil deforestation scenarios on the duration of the dry season in the arc of deforestation. *International Journal of Climatology*, *30*(13), 1970-1979. https://doi.org/10.1002/joc.2048

Cox, P. M. (2001). Description of the" TRIFFID" dynamic global vegetation model

Da Silva, R. R., Werth, D., & Avissar, R. (2008). Regional impacts of future land-cover changes on the Amazon basin wet-season climate. *Journal of climate*, *21*(6), 1153-1170. https://doi.org/10.1175/2007JCLI1304

Da Silva, H. J. F., Gonçalves, W. A., & Bezerra, B. G. (2019). Comparative analyzes and use of evapotranspiration obtained through remote sensing to identify deforested areas in the Amazon. *International Journal of Applied Earth Observation and Geoinformation*, *78*, 163-174. https://doi.org/10.1016/j.jag.2019.01.015

Da Silva, R. M., Lopes, A. G., & Santos, C. A. G. (2023). Deforestation and fires in the Brazilian Amazon from 2001 to 2020: Impacts on rainfall variability and land surface temperature. *Journal of Environmental Management*, *326*, 116664. https://doi.org/10.1016/j.jenvman.2022.116664.

Debortoli, N., Dubreuil, V., Hirota, M., Rodrigues Filho, S., Lindoso, D. P., & Nabucet, J. (2016). Detecting deforestation impacts in Southern Amazonia rainfall using rain gauges. *International Journal of Climatology*, *37*(6), 2889-2900. https://doi.org/10.1002/joc.4886

De Brito Gomes, W., Correia, F. W. S., Capistrano, V. B., Veiga, J. A. P., Vergasta, L. A., Chou, S. C., ... & Rocha, V. M. (2020). Water budget changes in the Amazon basin under RCP 8.5 and deforestation scenarios. *Climate Research*, *80*(2), 105-120. http://dx.doi.org/10.3354/cr01597

De Oliveira, A. P., & Fitzjarrald, D. R. (1994). The Amazon river breeze and the local boundary layer: II. Linear analysis and modelling. *Boundary-Layer Meteorology*, *67*(1), 75-96. https://doi.org/10.1007/BF00705508

De Oliveira, J. V., Ferreira, D. B. D. S., Sahoo, P. K., Sodré, G. R. C., de Souza, E. B., & Queiroz, J.C. B. (2018). Differences in precipitation and evapotranspiration between forested and deforested areas in the Amazon rainforest using remote sensing data. Environmental earth sciences, 77, 1-14.https:/doi.org/10.1007/s12665-018-7411- 9"https://doi.org/10.1007/s12665-018-7411-9

Dickinson, R. E., & Kennedy, P. (1992). Impacts on regional climate of Amazon deforestation. *Geophysical Research Letters*, *19*(19), 1947-1950. https://doi.org/10.1029/92GL01905

Doughty, C. E., Metcalfe, D. B., Girardin, C. A. J., Amézquita, F. F., Cabrera, D. G., Huasco, W. H., ... & Malhi, Y. (2015). Drought impact on forest carbon dynamics and fluxes in Amazonia. *Nature*, *519*(7541), 78-82. https://doi.org/10.1038/nature14213

Durieux, L., Machado, L. A. T., & Laurent, H. (2003). The impact of deforestation on cloud cover over the Amazon arc of deforestation. *Remote Sensing of Environment*, *86*(1), 132-140. https://doi.org/10.1016/S0034-4257(03)00095-6

Eiras-Barca, J., Dominguez, F., Yang, Z., Chug, D., Nieto, R., Gimeno, L., & Miguez-Macho, G. (2020). Changes in South American hydroclimate under projected Amazonian deforestation. *Annals of the New York Academy of Sciences*, *1472*(1), 104-122. https://doi.org/10.1111/nyas.14364

Eltahir, E. A., & Bras, R. L. (1994). Sensitivity of regional climate to deforestation in the Amazon basin. *Advances in Water Resources*, *17*(1-2), 101-115. https://doi.org/10.1016/0309-1708(94)90027-2

Ek, M. B., Mitchell, K. E., Lin, Y., Rogers, E., Grunmann, P., Koren, V., ... & Tarpley, J. D. (2003). Implementation of Noah land surface model advances in the National Centers for Environmental Prediction operational mesoscale Eta model. *Journal of Geophysical Research: Atmospheres*, *108*(D22). https://doi.org/10.1029/2002JD003296

Fels, S. B., & Schwarzkopf, M. D. (1975). The simplified exchange approximation: A new method for radiative transfer calculations. Journal of Atmospheric Sciences, 32(7), 1475-1488. https://doi.org/10.1175/1520-0469(1975)032%3C1475:TSEAAN%3E2.0.CO;2"2.0.CO;2

Fonseca, P., Veiga, J. A., Corrêa, F. W., Chan, C., & Lyra, A. (2017). An analysis of rainfall extremes in the Northern South America and their behaviors for future climate based on A1B scenario. *Revista Brasileira de Climatologia*, *20*. https://doi.org/10.5380/abclima.v20i0.47932

Gandu, A. W., Cohen, J. C. P., & De Souza, J. R. S. (2004). Simulation of deforestation in eastern Amazonia using a high-resolution model. *Theoretical and Applied Climatology*, *78*, 123-135. https://doi.org/10.1007/s00704-004-0048-5

Gash, J. H. C., & Nobre, C. A. (1997). Climatic effects of Amazonian deforestation: Some results from ABRACOS. Bulletin of the American meteorological society, 78(5), 823-830. https://doi.org/10.1175/1520-0477(1997)078%3C0823:CEOADS%3E2.0.C O;2"2.0.CO;2

INPE. (2017, January). *Projeto PRODES: Monitoring the Brazilian Amazon Forest by satellite.* São José dos Campos, Brazil. http://www.obt.inpe.br/prodes/index.php

INPE. (2022, January). *Monitoramento do Desmatamento da Floresta Amazônica Brasileira por Satélite.* PRODES-Amazônia. Taxa PRODES Amazônia 2004-2021 (km²). http://www.obt.inpe.br/OBT/assuntos/programas/amazonia/prodes

Hansen, J. E., & Lacis, A. A. (1974). A parameterization for the absorption of solar radiation in the earth's atmosphere. J Atmos Sci, 31, 118-133. https://doi. org/10.1175/1520-0469(1974)031%3C0118:APFTAO%3E2.0.CO;2"2.0.CO;2

Lean, J., & Rowntree, P. R. (1993). A GCM simulation of the impact of Amazonian deforestation on climate using an improved canopy representation. *Quarterly Journal of the Royal Meteorological Society*, *119*(511), 509-530. https://doi.org/10.1002/qj.49711951109

Lean, J., & Rowntree, P. R. (1997). Understanding the sensitivity of a GCM simulation of Amazonian deforestation to the specification of vegetation and soil characteristics. Journal of Climate, 10(6), 1216-1235. https://doi.org/10.1175/1520-0442(1997)010%3C1216:UTSOAG%3E2.0.CO;2"2.0.CO;2

Lean, J., & Warrilow, D. A. (1989). Simulation of the regional climatic impact of Amazon deforestation. *Nature*, *342*(6248), 411-413. https://doi.org/10.1038/342411a0

Leite-Filho, A. T., de Sousa Pontes, V. Y., & Costa, M. H. (2019). Effects of deforestation on the onset of the rainy season and the duration of dry spells in southern Amazonia. *Journal of Geophysical Research: Atmospheres*, *124*(10), 5268-5281. https://doi.org/10.1029/2018JD029537

Leite-Filho, A. T., Costa, M. H., & Fu, R. (2020). The southern Amazon rainy season: the role of deforestation and its interactions with large-scale mechanisms. *International Journal of Climatology*, *40*(4), 2328-2341. https://doi.org/10.1002/joc.6335

Lejeune, Q., Davin, E. L., Guillod, B. P., & Seneviratne, S. I. (2015). Influence of Amazonian deforestation on the future evolution of regional surface fluxes, circulation, surface temperature and precipitation. *Climate Dynamics*, *44*, 2769-2786. https://doi.org/10.1007/s00382-014-2203-8

Limberger, L., & Silva, M. E. S. (2016). Precipitação na bacia amazônica e sua associação à variabilidade da temperatura da superfície dos oceanos Pacífico e Atlântico: uma revisão. *GEOUSP Espaço e Tempo (Online)*, *20*(3), 657-675. https://doi.org/10.11606/issn.2179-0892.geousp.2016.105393

Llopart, M., Reboita, M. S., Coppola, E., Giorgi, F., Da Rocha, R. P., & De Souza, D. O. (2018). Land use change over the Amazon Forest and its impact on the local climate. *Water*, *10*(2), 149. https://doi.org/10.3390/w10020149

Marengo, J. A. (2006). On the hydrological cycle of the Amazon Basin: A historical review and current state-of-the-art. *Revista brasileira de meteorologia*, *21*(3), 1-19

Marengo, J. A., & Espinoza, J. C. (2016). Extreme seasonal droughts and floods in Amazonia: causes, trends and impacts. *International Journal of Climatology*, *36*(3). https://doi.org/10.1002/joc.4420

Mellor, G. L., & Yamada, T. (1974). A hierarchy of turbulence closure models for planetary boundary layers. Journal of the atmospheric sciences, 31(7), 1791-1806. https://doi.org/10.1175/1520-0469(1974)031%3C1791:AHOTCM%3E2.0.C O;2"2.0.CO;2

Mesinger, F. (1984). A blocking technique for representation of mountains in atmospheric models. *Riv. Meteorol. Aernonaut.*, *44*, 195-202

Mesinger, F., Chou, S. C., Gomes, J. L., Jovic, D., Bastos, P., Bustamante, J. F., ... & Veljovic, K. (2012). An upgraded version of the Eta model. *Meteorology and Atmospheric Physics*, *116*, 63-79. https://doi.org/10.1007/s00703-012-0182-z

Moreira, R. M. (2024). Trends and correlation between deforestation and precipitation in the Brazilian Amazon Biome. *Theoretical and Applied Climatology*, *155*(5), 3683-3692. https://doi.org/10.1007/s00704-024-04838-5

Mota, M., & Souza, P. (1996). Influência da precipitação nas características termodinâmicas da atmosfera durante um mês seco. In *CONGRESSO BRASILEIRO DE METEOROLOGIA* (Vol. 9, pp. 1136-1138)

Mu, Y., & Jones, C. (2022). An observational analysis of precipitation and deforestation age in the Brazilian Legal Amazon. *Atmospheric Research*, *271*, 106122. https://doi.org/10.1016/j.atmosres.2022.106122

Nobre, C. A., Sellers, P. J., & Shukla, J. (1991). Amazonian deforestation and regional climate change. Journal of climate, 4(10), 957-988. https://doi.org/10.1175/1520-0442(1991)004%3C0957:ADARCC%3E2.0.CO;2"2.0.CO;2

Nobre, C. A., Sampaio, G., & Salazar, L. (2007). Mudanças climáticas e Amazônia. *Ciência e Cultura*, *59*(3), 22-27

O'Connor, F. M., Johnson, C. E., Morgenstern, O., Abraham, N. L., Braesicke, P., Dalvi, M., ... & Pyle, J. A. (2014). Evaluation of the new UKCA climate-composition model–Part 2: The Troposphere. *Geoscientific Model Development*, *7*(1), 41-91. https://doi.org/10.5194/gmd-7-41-2014

O'Connor, J. C., Santos, M. J., Dekker, S. C., Rebel, K. T., & Tuinenburg, O. A. (2021). Atmospheric moisture contribution to the growing season in the Amazon arc of deforestation. *Environmental Research Letters*, *16*(8), 084026. https://doi.org/HYPERLINK "https://doi.org/10.1088/1748-9326/ac12f0"10.1088/1748-9326/ac12f0

Palmer, J. R., & Totterdell, I. J. (2001). Production and export in a global ocean ecosystem model. *Deep Sea Research Part I: Oceanographic Research Papers*, *48*(5), 1169-1198. https://doi.org/10.1016/S0967-0637(00)00080-7

Reboita, M. S., Gan, M. A., Rocha, R. P. D., & Ambrizzi, T. (2010). Regimes de precipitação na América do Sul: uma revisão bibliográfica. *Revista brasileira de meteorologia*, *25*, 185-204. https://doi.org/10.1590/S0102-77862010000200004

Rocha, V. M., Correia, F. W. S., Satyamurty, P., de Freitas, S. R., Moreira, D. S., da Silva, P. R. T., & Fialho, E. S. (2014). Impacts of land cover and greenhouse gas (GHG) concentration changes on the hydrological cycle in amazon basin: a regional climate model study. *Revista Brasileira de Climatologia*, *15*. https://doi.org/10.5380/abclima.v15i0.36386

Rocha, V. M. (2016). Avaliação dos impactos das mudanças climáticas na reciclagem de precipitação da Amazônia: Um estudo de modelagem numérica. *Revista Brasileira de Climatologia*, *19*. https://doi.org/10.5380/abclima.v19i0.48875

Rocha, V. M., Correia, F. W. S., & Gomes, W. B. (2019). Avaliação dos impactos da mudança do clima na precipitação da Amazônia utilizando o modelo RCP 8.5 Eta-HadGEM2-ES. *Revista Brasileira de Geografia Física*, *12*(06), 2051-2065. https://doi.org/10.26848/rbgf.v12.6.p2051-2065

Rodriguez, D. A., Chou, S. C., Tomasella, J., & Demaria, E. M. (2014). Impacts of landscape fragmentation on simulated precipitation fields in the Amazonian sub-basin of Ji-Paraná using the Eta model. *Theoretical and applied climatology*, *115*, 121-140. https://doi.org/10.1007/s00704-013-0866-4

S. Debortoli, N., Dubreuil, V., Funatsu, B., Delahaye, F., De Oliveira, C. H., Rodrigues-Filho, S., ... & Fetter, R. (2015). Rainfall patterns in the Southern Amazon: a chronological perspective (1971–2010). *Climatic Change*, *132*, 251-264. https://doi.org/10.1007/s10584-015-1415-1

Salati, E., Dall'Olio, A., Matsui, E., & Gat, J. R. (1979). Recycling of water in the Amazon basin: an isotopic study. *Water resources research*, *15*(5), 1250-1258. https://doi.org/10.1029/WR015i005p01250

Sampaio, G., Nobre, C., Costa, M. H., Satyamurty, P., Soares-Filho, B. S., & Cardoso, M. (2007). Regional climate change over eastern Amazonia caused by pasture and soybean cropland expansion. *Geophysical Research Letters*, *34*(17). https://doi.org/10.1029/2007GL030612

Sampaio, G., Shimizu, M., Guimarães-Júnior, C. A., Alexandre, F., Cardoso, M., Domingues, T. F., ... & Lapola, D. M. (2020). CO 2 fertilization effect can cause rainfall decrease as strong as large-scale deforestation in the Amazon. *Biogeosciences Discussions*, *2020*, 1-21. https://doi.org/10.5194/bg-18-2511-2021

Sestini, M. F., ALVALÁ, R. D. S., Mello, E. M. K., VALERIANO, D. D. M., Chan, C. S., Nobre, C. A., ... & REIMER, E. D. S. (2002). Elaboração de mapas de vegetação para utilização em modelos meteorológicos e hidrológicos. *São José dos Campos: INPE*, 74

Silva, M. E. S., Pereira, G., & da Rocha, R. P. (2016). Local and remote climatic impacts due to land use degradation in the Amazon "Arc of Deforestation". *Theoretical and Applied Climatology*, *125*, 609-623. https://doi.org/10.1007/s00704-015-1516-9

Shukla, J., Nobre, C., & Sellers, P. (1990). Amazon deforestation and climate change. *Science*, *247*(4948), 1322-1325. https://doi.org/10.1126/science.247.4948.1322

Soares-Filho, B., Alencar, A., Nepstad, D., Cerqueira, G., Vera Diaz, M. D. C., Rivero, S., ... & Voll, E. (2004). Simulating the response of land-cover changes to road paving and governance along a major Amazon highway: the Santarém−Cuiabá corridor. *Global change biology*, *10*(5), 745-764. https://doi.org/10.1111/j.1529-8817.2003.00769.x

Zhao, Q., Black, T. L., & Baldwin, M. E. (1997). Implementation of the cloud prediction scheme in the Eta Model at NCEP. Weather and Forecasting, 12(3), 697-712. https://doi.org/10.1175/1520-0434(1997)012%3C0697:IOTCPS%3E2.0.CO;2"2.0.CO;2

Authorship contributions

1 – Karoline Suelly de Souza Mendes

Master's degree student in the Climate and Environment Postgraduate Program at the National Institute for Amazon Research/University of the State of Amazonas
https://orcid.org/0009-0002-9127-4092 • ksdsm.mcl23@uea.edu.br
Contribution: Formal analysis, Investigation, Methodology, Software, Writing – original draft and Writing - review & editing

2 – Adriane Lima Brito

Master's and Ph.D. in Climate and Environment from the National Institute for Amazon Research (INPA)
https://orcid.org/0000-0002-9492-273X • meteorologia.dri@gmail.com
Contribution: Data curation, Methodology, Software, Validation, Visualization and Writing - review & editing

3 – Adriana Lira Lima

Ph.D. student in the Climate and Environment Postgraduate Program at the National Institute of Amazon Research.
https://orcid.org/0000-0001-7686-2115 • all.dcl23@uea.edu.br
Contribution: Software, Validation, Visualization, Writing – review & editing

4 – José Augusto Paixão Veiga

Ph.D. in Meteorology from the National Institute for Space Research (INPE).
https://orcid.org/0000-0001-5214-5349 • jveiga@uea.edu.br
Contribution: Conceptualization, Data curation, Funding acquisition, Methodology, Project administration, Resources, Supervision, Validation and Visualization.

How to quote this article

Mendes, K. S. de S., Brito, A. L., Lima, A. L., & Veiga, J. A. P. (2024). How has deforestation affected and might affect the climate in the Amazon Basin during the rainy season? *Ciência e Natura*. 46, e85441. https://doi.org/10.5902/2179460X85441